Acta Crystallographica Section D
Biological Crystallography
ISSN 0907-4449

Structure of *Escherichia coli* pyruvate formate-lyase with pyruvate

Lari Lehtiö,[a] Veli-Matti Leppänen,[a] John W. Kozarich[b] and Adrian Goldman[a]*

[a]Institute of Biotechnology, University of Helsinki, PO Box 65, FIN-00014, Helsinki, Finland, and [b]ActivX Biosciences Inc., 11025 North Torrey Pines Road, Suite 120, La Jolla, CA 92037, USA

Correspondence e-mail: adrian.goldman@helsinki.fi

Received 17 May 2002
Accepted 10 September 2002

PDB Reference: pyruvate formate lyase–pyruvate complex, 1mzo, r1mzosf.

The structure of inactive pyruvate formate-lyase in complex with a natural substrate, pyruvate, was solved at 2.7 Å resolution. Both active sites of the homodimeric enzyme are occupied by pyruvate; additional binding sites were not found. Pyruvate was found in a cleft close to the active-site cysteines 418 and 419, with the carboxyl group in contact with arginines 176 and 435 and the methyl group within van der Waals distance of Phe327. It is believed that the binding site of pyruvate is not the position of pyruvate as the reaction initiates, as conformational changes occur during activation of the enzyme.

1. Introduction

Pyruvate formate-lyase (PFL; EC 2.3.1.54) is an anaerobic enzyme that catalyses the conversion of pyruvate and coenzyme A (CoA) to acetyl-CoA and formate. PFL is a homodimer of 85 kDa subunits, displaying half-of-the-sites reactivity (Unkrig *et al.*, 1989). Active PFL contains a relatively stable glycyl radical located at Gly734 (Knappe *et al.*, 1984; Wagner *et al.*, 1992). Activation of PFL is performed by an activating enzyme (EC 1.97.1.4) containing an iron–sulfur cluster, which generates the Gly734 radical using a 5′-deoxyadenosyl radical derived from *S*-adenosyl methionine (Frey *et al.*, 1994). Pyruvate, or its analogue oxamate, is required for activation (Chase & Rabenowitz, 1968; Knappe *et al.*, 1974).

Based on numerous biochemical studies, various mechanistic models have been proposed (reviewed by Stubbe & van der Donk, 1998). Several well established features of the mechanism include the Gly734 radical, involvement of Cys418 and Cys419 close to Gly734 (Plaga *et al.*, 1988) and hydrogen exchange between Cys419 and Gly734 (Parast *et al.*, 1995). Pyruvate (or oxamate) is required for activation of PFL, but it is not clear whether pyruvate binds first to the active site of PFL in the kinetic pathway, with subsequent activation of the Gly radical, or whether the 'activating pyruvate' binds elsewhere and pyruvate only binds in the active site subsequent to activation. Recent crystal structures (Leppänen, Merckel *et al.*, 1999; Becker *et al.*, 1999) have elucidated features supporting the mechanistic models. PFL contains a ten-stranded α/β-barrel which consists of two sets of five parallel β-strands assembled in an antiparallel manner. Inside the barrel is a loop containing the active-site cysteines. These features relate PFL to another class of radical enzymes, the ribonucleotide reductases (RNRs; Uhlin & Eklund, 1994; Logan *et al.*, 1999). In PFL there is also another loop containing Gly734 inside the barrel. This loop is also present in class III RNRs, which likewise work anaerobically *via* a glycyl radical. Based on the PFL–oxamate complex structure, Becker *et al.* (1999) proposed that the thiyl radical Cys418 attacks the substrate, although we have suggested Cys419 as the attacking radical (Wong & Kozarich, 1994; Leppänen *et al.*, 1999) based on previous work from the Knappe group (Plaga *et al.*, 1988; Knappe & Wagner, 1995). Oxamate, however, is an inert analogue of pyruvate (with an amino group in place of the methyl group) that is believed not to bind to the active site (Knappe *et al.*, 1974). Here, we report the binding of pyruvate in a manner similar to that of oxamate. This result throws some doubt on oxamate-bound models of catalysis (Becker *et al.*, 1999).

2. Materials and methods

2.1. Purification and crystallization

Recombinant PFL was purified from *Escherichia coli* BL21 (DE3) (Pharmacia) bearing pKKBWM5.5C (Parast *et al.*, 1995). Induction with IPTG was not required. Cell culture and protein purification were performed as published for a stable proteolytic fragment of PFL (Leppänen, Parast *et. al.*, 1999). Only a single anion-exchange step was required to achieve crystallizable protein.

After anion exchange, fractions containing PFL were pooled and the buffer was changed with multiple concentration and dilution steps to 50 m*M* MOPS/NH_3 containing 20 m*M* DTT. Finally, PFL was concentrated to 25 mg ml^{-1} with Centriprep-30 (Amicon). Protein concentrations were determined with a Bio-Rad kit (Bradford, 1976) with bovine serum

Table 1
Summary of data processing.

Values in parentheses are for the highest resolution shell.

Resolution (Å)	20–2.7 (2.8–2.7)
Wavelength (Å)	0.9102
No. of observations	318766
No. of unique reflections	55923
Space group	$P4_32_12$
Unit-cell parameters (Å)	$a = b = 158.36$, $c = 159.30$
Completeness (%)	98.8 (94.9)
R_{sym}† (%)	11.1 (34.0)
$I/\sigma(I)$	8.9 (1.5)

† $R_{sym} = \sum_i |I_i - \langle I \rangle| / \sum \langle I \rangle$, where I is an individual intensity measurement and $\langle I \rangle$ is the average intensity for this reflection, with summation over all data.

Table 2
Summary of refinement statistics.

No. of atoms	
Total	12470
Protein	11930
Pyruvate	12
Water	518
Polyethylene glycol	10
Mean atomic displacement parameters (Å^2)	
Total	46.7
Protein	47.1
Pyruvate	41.1
Water	36.2
PEG	56.7
R factor† (%)	19.6
R_{free}‡ (%)	23.5
R.m.s. deviations	
Bond lengths (Å)	0.007
Bond angles (°)	1.2
Dihedral angles (°)	21.5
Improper angles (°)	0.72
Ramachandran plot	
Residues in most favoured regions (%)	87.0
Residues in additional allowed regions (%)	12.4
Residues in generously allowed regions (%)	0.4
Residues in disallowed regions (%)	0.1

† R factor is defined as $\sum ||F_{obs}| - |F_{calc}|| / \sum |F_{obs}|$, where F_{obs} and F_{calc} are the observed and calculated structure-factor amplitudes, respectively. ‡ R free is the R factor for the test set (5% of the data).

albumin as a standard. Crystallization was accomplished essentially as reported by Becker *et al.* (1999). Crystals were obtained from 50 µl dialysis buttons (Hampton Research) placed in a well containing 1.5 ml 25 m*M* MOPS/NH_3 pH 7.3, 25%(*w*/*v*) PEG 1000, 10 m*M* DTT, 25 m*M* NH_4Cl, 25 m*M* sodium pyruvate, 1 m*M* EDTA and 2 m*M* $MgCl_2$. Crystals grew to dimensions of 0.6 × 0.5 × 0.5 mm within a week and were stored at a higher PEG concentration [30%(*w*/*v*)].

2.2. Data collection and refinement

Prior to data collection, crystals were dialysed overnight against 25 m*M* MOPS/NH_3 pH 7.3 containing 30%(*w*/*v*) PEG 1000, 25 m*M* NH_4Cl, 25 m*M* sodium pyruvate, 10 m*M* DTT and 1 *M* DL-threitol. Crystals were then picked up in a loop and frozen in liquid nitrogen. Synchrotron radiation was used for data collection on the X11 beamline at the EMBL Outstation, DESY (Hamburg, Germany) equipped with a MAR CCD detector. Diffraction data were processed using the *HKL* package (Otwinowski & Minor, 1997) and the statistics are given in Table 1. Molecular-replacement methods were used to solve the structure at 4 Å resolution using the PFL structure as a search model (Becker *et al.*, 1999; PDB code 2pfl). The resolution was extended to 2.7 Å in several rounds of rigid-body refinement with monomers defined as rigid bodies. 5% of the data was excluded from refinement for free *R*-factor calculation. Molecular replacement and refinement were performed with *CNS* (Brünger *et al.*, 1998). Non-crystallographic symmetry restraints with a weight of 500 between monomers were applied throughout the refinement. Part of a PEG molecule was modelled between symmetry-related dimers. Refinement statistics are shown in Table 2. The stereochemical correctness of the protein model was verified with *PROCHECK* (Laskowski *et al.*, 1993).

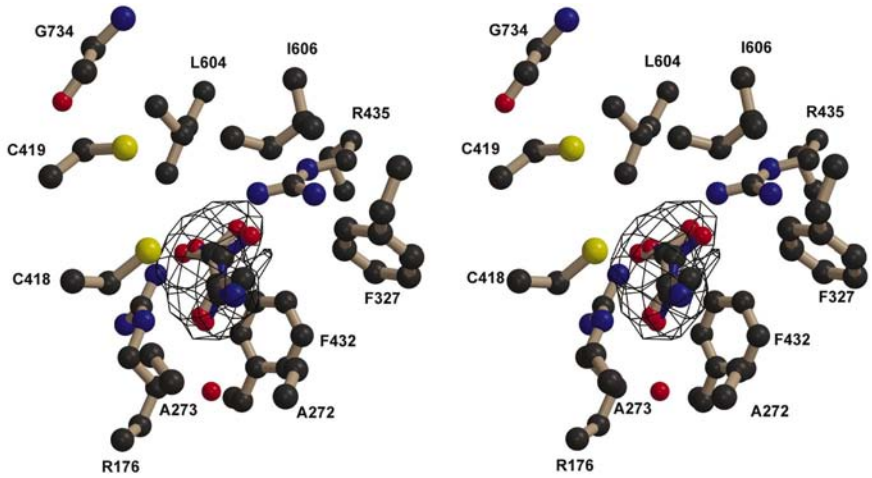

Figure 1
Comparison of pyruvate and oxamate binding to the active site of PFL. The side chains of surrounding residues and the main-chain atoms of Gly734 of the PFL–pyruvate complex are shown. Residues of the oxamate structure (taken from the 3pfl coordinates in the PDB) and Trp333 are omitted for clarity. Oxamate is coloured blue. Electron density of the $F_o - F_c$ omit map contoured at 5σ is shown around pyruvate. The figure was produced with *BOBSCRIPT* (Esnouf, 1997) and *Raster3D* (Merritt & Murphy, 1994).

3. Results and discussion

The root-mean-square deviation between the PFL–pyruvate complex and the oxamate complex is 0.30 Å per C^{α}. Electron-density peaks above 10σ in the $F_o - F_c$ map could be identified as pyruvate molecules in both active sites. Although it was shown by Knappe & Wagner (1995) that only one pyruvate molecule is bound covalently per PFL dimer whether it is active or inactive, here we show that both active sites are equally occupied. Electron density between Cys418 and the carbonyl carbon of pyruvate is continuous, but thiohemiketal as a covalent adduct does not fit the density properly, even though Knappe & Wagner (1995) reported that a single thiohemiketal is bound per monomer in the inactive enzyme to Cys419 not Cys418 – results we have been unable to reproduce (Kozarich, unpublished work). An electron-density map calculated without pyruvate shows good density around the substrate, indicating that in this structure pyruvate is closer to Cys418 than Cys419, with carbonyl carbon–sulfur distances of 3.0 and 5.8 Å, respectively (Fig. 1). Additional pyruvate molecules were not found. Pyruvate is bound to a cleft between arginines 176 and 435. Oxamate was also modelled between the two arginines (Becker *et al.*, 1999), but there is a rotation of 18° between these molecules (Fig. 1). The largest difference between equivalent atoms in pyruvate and oxamate is 0.8 Å (carboxyl O atoms). This rotation is caused by hydrophobic interactions between the methyl group of pyruvate and hydrophobic residues surrounding the active site (Fig. 2), which cannot occur with the oxamate amino group. In particular, the distance between Phe327 and the pyruvate methyl group, replaced by the amino group in oxamate, has decreased from 4.4 to 3.6 Å.

A PEG molecule was found between symmetry-related dimers. Previous structures have described this site as consisting of water molecules, but the density in our structure clearly supports a part of a PEG molecule ($C_{12}O_7$). PEG plays a crucial role in the crystallization of PFL by binding to a cleft formed by two symmetry-related dimers.

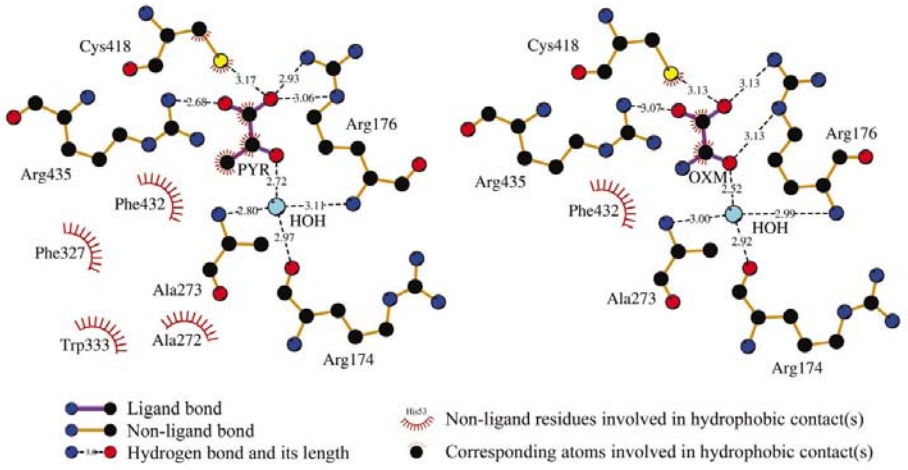

Figure 2
Two-dimensional plots of residues that interact with pyruvate and oxamate (from 3pfl). Residues forming hydrogen bonds with pyruvate or oxamate and residues contibuting to hydrophobic interaction are shown. Distances are in ångströms. The figure was produced with *HBPLUS* (McDonald & Thornton, 1994) and *LIGPLOT* (Wallace *et al.*, 1995).

All the structural studies were performed with inactive PFL and we believe that large-scale conformational changes occur during activation. Firstly, all the structures solved are symmetric, but PFL has half-of-the-sites reactivity, as only one of the two Gly734 residues forms a radical (Unkrig *et al.*, 1989). Secondly, the glycine loop is buried in the inactive enzyme inside the ten-stranded barrel about 8 Å from the surface, so either a radical transfer chain, as in ribonucleotide reductase type I (Stubbe & van der Donk, 1998), or else a conformational change involving a large-scale motion of the Gly loop must occur. The latter is clearly correct, as H-atom transfer occurs directly from Gly734 to the adenosyl radical (Frey *et al.*, 1994). However, there are essentially no changes between the apo-oxamate and pyruvate structures (Gly734 C^{α} moves by 0.25 Å between the apo and the oxamate-complex structure and by 0.2 Å between the apo and the pyruvate-complex structure), making it hard to see how the inactive pyruvate-complex and oxamate-complex structures could undergo activation. Thirdly, oxamate works as an effector enabling the activation to occur, but it should not bind to the active site of *active* PFL (Knappe *et al.*, 1974). Finally, the oxamate structure (Becker *et al.*, 1999) and our pyruvate complex structures show no signs of a CoA-binding pocket leading to the active site. Consequently, it is hard to make direct conclusions about the mechanism based on these structures.

One possibility (as discussed in Becker *et al.*, 1999) is that these structures reveal the position of pyruvate and oxamate as the allosteric activator at or close to the site of catalysis. Another possibility is that the site described here (and in Becker *et al.*, 1999) represents adventitious binding arising from the non-physiological concentration (25 m*M*) of pyruvate used. In that case, it is unclear where pyruvate and oxamate bind to PFL as allosteric activators. An intriguing possibility remains, therefore, that the allosteric site is not on PFL, but is instead on the activating enzyme (Knappe *et al.*, 1974). The catalytic mechanism we originally proposed (Leppänen, Merckel *et al.*, 1999; Wong & Kozarich, 1994; Brush *et al.*, 1988) could still be correct: the site of radical attack could be at Cys419 although, on balance, the structures are more consistent with attack by Cys418. If attack were at Cys419, pyruvate would have to move by a few ångströms from its current position.

Based on the structure of a stable proteolytic fragment of PFL, we proposed that coenzyme A (CoA) binds to a cleft surrounded by Arg313 and Arg316 (Leppänen, Merckel *et al.*, 1999). With respect to the full-length protein, this seems still to be possible: arginines 107, 313, 316 and 738 and Asn65 form a pocket that could bind the polar head group of CoA. For CoA to bind, however, a conformational change is required. The fact that a conformational change is required is consistent with solution data showing that CoA-mediated thioester exchange is slow in the unactivated enzyme (Knappe *et al.*, 1993) and with the structural and biochemical data (above) indicating that the active site in this structure is not in the active conformation. Clearly, a full picture of catalysis in PFL will only emerge from structures of the activated enzyme.

Note added in proof: The CoA binding mode described in a recent paper is different than the one discussed here (Becker & Kabcsh, 2002).

This work was supported by a grant from Merck Research Laboratories and by the general facilities of the Institute of Biotechnology, Helsinki. We thank EMBL for access to the X11 synchtrotron beamline under the European Union access to research infrastructure action of the improving human potential programme: HPRI-CT-1999-00017. We also thank Dr Michael Merckel for helpful discussions and Markus Tujula for help with the computers.

References

Becker, A., Fritz-Wolf, K., Kabsch, W., Knappe, J., Schultz, S. & Volker Wagner, A. F. (1999). *Nature Struct. Biol.* **6**, 969–975.
Becker, A. & Kabsch, W. (2002). *J. Biol. Chem.* **277**, 40036–40042.
Bradford, M. M. (1976). *Anal. Biochem.* **72**, 248–254.
Brünger, A. T., Adams, P. A., Clore, G. M., DeLano, W. L., Gros, P., Grosse-Kunstleve, R. W., Jiang, J.-S., Kuszewski, J., Nilges, M., Pannu, N. S., Read, R. J., Simonson, T. & Warren, G. L. (1998). *Acta Cryst.* D**54**, 905–921.
Brush, E. J., Lipsett, K. A. & Kozarich, J. W. (1988). *Biochemistry*, **27**, 2217–2222.
Chase, T. Jr & Rabenowitz, J. C. (1968). *J. Bacteriol.* **96**, 1065–1078.
Esnouf, R. M. (1997) *J. Mol. Graph.* **15**, 132–134.
Frey, M., Rothe, M., Wagner, A. F. & Knappe, J. (1994). *J. Biol. Chem.* **269**, 12432–12437.
Knappe, J., Blaschkowski, H. P., Gröbner, P. & Schmitt, T. (1974). *Eur. J. Biochem.* **50**, 253–263.
Knappe, J., Elbert, S., Frey, M. & Wagner, A. F. V. (1993). *Biochem. Soc. Trans.* **21**, 731–734.
Knappe, J., Neugebauer, F. A., Blaschkowski, H. P. & Ganzler, M. (1984). *Proc. Natl Acad. Sci. USA*, **81**, 1332–1335.
Knappe, J. & Wagner, A. F. (1995). *Methods Enzymol.* **258**, 343–362.
Laskowski, R. A., MacArthur, M. W., Moss, D. S. & Thornton, J. M. (1993). *J. Appl. Cryst.* **26**, 283–291.
Leppänen, V.-M., Merckel, M. C., Ollis, D. L., Wong, K. K., Kozarich, J. W. & Goldman, A. (1999). *Structure Fold. Des.* **7**, 733–744.
Leppänen, V.-M., Parast, C. V., Wong, K. K., Kozarich, J. W. & Goldman, A. (1999*b*). *Acta Cryst.* D**55**, 531–533.
Logan, T. L., Andersson, J., Sjöberg, B.-M. & Nordlund, P. (1999). *Science*, **283**, 1499–1504.
McDonald, I. K. & Thornton, J. M. (1994). *J. Mol. Biol.* **238**, 777–793.
Merritt, E. A. & Murphy, M. E. P. (1994). *Acta Cryst.* D**50**, 869–873.
Otwinowski, Z. & Minor, W. (1997). *Methods Enzymol.* **276**, 307–326.
Parast, C. V., Wong, K. K., Lewisch, S. A., Kozarich, J. W., Peisach, J. & Magliozzo, R. S. (1995). *Biochemistry*, **34**, 2393–2399.
Plaga, W., Frank, R. & Knappe, J. (1988). *Eur. J. Biochem.* **178**, 445–450.
Stubbe, J. & van der Donk, W. A. (1998). *Chem. Rev.* **98**, 705–762.

Uhlin, U. & Eklund, H. (1994). *Nature (London)*, **370**, 533–539.
Unkrig, V., Neugebauer, F. A. & Knappe, J. (1989). *Eur. J. Biochem.* **184**, 723–728.
Wagner, A. F., Frey, M., Neugebauer, F. A., Schafer, W. & Knappe, J. (1992). *Proc. Natl Acad. Sci. USA*, **89**, 996–1000.
Wallace, A. C., Laskowski, R. A. & Thornton, J. M. (1995). *Protein Eng.* **8**, 127–134.
Wong, K. K. & Kozarich, J. W. (1994). *Metal Ions in Biological Systems*, edited by H. Sigel, pp. 279–313. New York: Marcel Dekker Inc.